



# Geochronology, paleomagnetism and magnetic fabric of metamorphic rocks in the northeast Fraser Belt, Western Australia\*

B. DE WAELE<sup>†</sup> AND S. A. PISAREVSKY<sup>‡</sup>

*Tectonics Special Research Centre, University of Western Australia, 35 Stirling Highway, Crawley, WA 6009 Australia.*

The first zircon U–Pb SHRIMP dating on high-grade meta-igneous units in the northernmost parts of the Fraser Belt along the southern margin of the Western Australian Yilgarn Craton, reveal crystallisation ages between  $1299 \pm 10$  and  $1250 \pm 23$  Ma. A small number of older xenocrystic zircons, incorporated in some samples, indicate the presence of Late Paleoproterozoic crust in the region. Zircon that crystallised within a melt accumulated in the neck of a boudinaged mafic unit was dated at  $1296 \pm 4$  Ma, indicating that the emplacement of the igneous protoliths took place syntectonically. The anisotropy of magnetic susceptibility of the granulites indicates minimum axes with a mean inclination of  $4^\circ$  towards  $130^\circ$ , corresponding to a nearly vertical southwest–northeast ( $50$ – $230^\circ$ ) magnetic foliation. This is very close to the structural trend of the Fraser Belt suggesting that the magnetic fabric was acquired syntectonically, during the collision between the Yilgarn and Gawler Cratons. The paleomagnetic data on the granulites overlap with published poles for various 1.2 Ga units in the Albany Belt and the 1.2 Ga Fraser dykes, possibly suggesting that the remanence was acquired during the second stage of the Fraser tectonism. A younger magnetisation component resembles a pole of uncertain age published for Bremer Bay in the Albany Belt.

**KEY WORDS:** Fraser Belt, geochronology, magnetic fabric, metamorphic rocks, paleomagnetism, SHRIMP, uranium–lead dating, Western Australia, zircon.

## INTRODUCTION

The Albany–Fraser Orogen is a Mesoproterozoic belt that occurs along the southern and southeastern margins of the Archean (3000–2600 Ma) Yilgarn Craton of Western Australia (Figure 1, inset). The belt is considered a curvilinear collision zone between the Yilgarn Craton and East Antarctica (Mawson Land) to form the Albany Belt, and collision between the Yilgarn Craton and the Gawler Craton to form the Fraser Belt (Dawson *et al.* 2002; Fitzsimons 2003). Because of the fact that tectonism in the Albany–Fraser Orogen is believed to be coeval across the entire orogen, it is generally assumed that the Gawler and East Antarctic blocks formed a coherent cratonic unit called the Mawson Craton (Myers 1993), which collided *en masse* with the Yilgarn Craton. Moreover, based on broad similarities in the tectonothermal events recognised in the central Australian Musgrave Complex (Camacho & Fanning 1995; Camacho *et al.* 1997; Camacho & McDougall 2000), and

those occurring in the Albany–Fraser Orogen (Nelson *et al.* 1995; Clark *et al.* 2000), it has been suggested that this collision involved a West Australian–North Australian cratonic assemblage, with the formation of a Pan-Australian Mesoproterozoic orogen we will refer to as the Albany–Fraser–Musgrave Orogen.

To date, geochronological data cover only the Albany Belt and southernmost parts of the Fraser Belt, while parts of the Musgrave Complex have only very recently attracted scientific interest (Howard *et al.* 2005), resulting in a patchy geochronological database precluding detailed correlation. This paper presents new zircon U–Pb geochronological data for the northernmost parts of the Fraser Complex (north of  $30^\circ\text{S}$ ) and associated gneisses, providing a robust geochronological framework for this part of the orogen.

Previous paleomagnetic studies in the Albany Belt (Pisarevsky & Harris 2001; Pisarevsky *et al.* 2003) revealed two stable remanence components. The predominant steep remanence corresponds to *ca* 1200 Ma,

\*Appendix 1 [indicated by an asterisk (\*) in the text and listed at the end of the paper] is a Supplementary Paper; copies may be obtained from the Geological Society of Australia's website (<<http://www.gsa.org.au>>) or from the National Library of Australia's Pandora archive (<<http://nla.gov.au/nla.arc-25194>>).

<sup>†</sup>Corresponding author and present address: British Geological Survey, Kingsley Dunham Centre, Keyworth NG12 5GG, UK (bdewaele@bgs.ac.uk).

<sup>‡</sup>Present address: School of Geosciences, University of Edinburgh, Grant Institute, The King's Buildings, West Mains Road, Edinburgh EH9 3JW, UK.

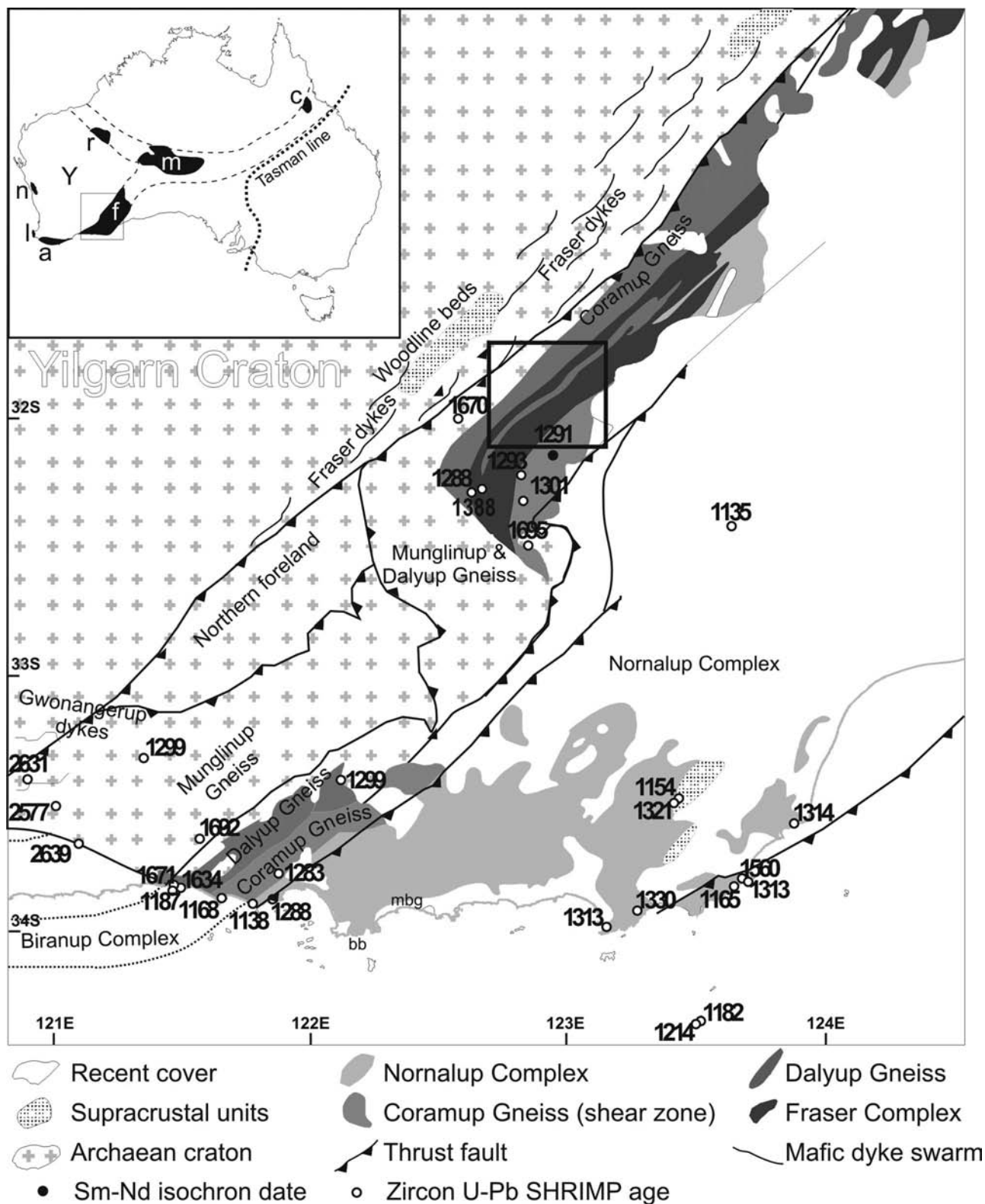


**Figure 1** Simplified map of the southern part of the Fraser Belt indicating published age data (based on Myers 1990, Fitzsimons & Buchan 2005, Spaggiari *et al.* 2007). bb, Bremer Bay; mbg, approximate location of the Mt Barren Group. Inset shows the location of Mesoproterozoic tectonic units of Australia (n, Northampton Complex; l, Leeuwin Complex; a, Albany Belt; f, Fraser Belt; m, Musgrave Complex; c, Cape River and Iron Range Province: after Spaggiari *et al.* 2007). The box indicates the extent of Figure 2.

while the age of the second shallow southeast component is unclear. Here we expand paleomagnetic and anisotropy of magnetic susceptibility (AMS) studies to

the northeast, presenting the results of reconnaissance investigations on the granulite-grade metamorphic rocks of the Fraser Complex.

## GEOLOGICAL BACKGROUND OF THE ALBANY–FRASER OROGEN

The Albany–Fraser Belt is dominated by granulite-grade paragneiss and orthogneiss intruded by late-tectonic granite plutons in the west (Albany Belt), and by orthogneiss and mafic granulite in the east (Fraser Belt including the Fraser Complex). These high-grade units are overlain by a series of low-grade metasedimentary successions dominated by quartzite and metapelite. The Albany–Fraser Orogen has been subdivided into a series of tectonic terranes, based on terrane-bounding faults and distinct lithotectonic character (Figure 1). These include the structurally and thermally reworked southern margin of the Yilgarn Craton, which comprises amphibolite facies orthogneiss intruded by margin-parallel dykes of the Gnowangerup and Fraser Dyke swarms (Evans 1999; Wingate *et al.* 2000). To the south of the craton, the Biranup Complex occurs, which comprises reworked portions of the Yilgarn Craton, the felsic Munglinup Gneiss, with protolith ages in the range 2640–2575 Ma. The remainder of the Biranup Complex comprises the Dalyup Gneiss with protolith ages in the range 1700–1630 Ma and the high-strain Coramup Gneiss derived through shearing of the Dalyup Gneiss (Clark 1995; Nelson *et al.* 1995; Clark *et al.* 1999, 2000; Bodorkos & Clark 2004a, b). Those latter units are regarded as representing exotic fragments accreted to the Yilgarn Craton (Spaggiari *et al.* 2007). Outboard of the Biranup Complex, the Nornalup Complex occurs which comprises both orthogneiss and paragneiss units dated at >1450 Ma (Myers 1995) and intruded by granitoids in the age range 1330–1280 Ma and 1190–1135 Ma (Nelson *et al.* 1995). To the east, the Fraser Complex occurs, comprising granulite-grade mafic and felsic orthogneisses dated at 1300–1280 Ma (Fletcher *et al.* 1991; Clark 1995; Condie & Myers 1999; Clark *et al.* 1999, 2000). These various tectonic complexes are presumed to represent allochthonous terranes, including oceanic arc (Fraser Complex: Condie & Myers 1999) and continental arc or micro-continental terranes (Fitzsimons 2003).

### Geochronological framework for the Albany–Fraser Orogen

Because of its remote location and a general lack of economic interest, the Fraser Orogen had remained poorly studied until recent years. Various Rb–Sr and Sm–Nd isotopic data on the northeastern part of the Fraser Orogen, summarised by Fletcher *et al.* (1991), indicated that the Yilgarn Craton foreland to the orogen had not been metamorphosed above the amphibolite facies since *ca* 1.6 Ga, while the Fraser Complex itself appeared to have undergone granulite-facies metamorphism at *ca* 1.3 Ga. The lack of a thermal overprint onto the Yilgarn margin at *ca* 1.3 Ga was interpreted to suggest that the Fraser Complex was at least partially cooled prior to its juxtaposition with the Yilgarn Craton. However, the recent recognition of large portions of reworked Yilgarn Craton (Munglinup Gneiss: Spaggiari *et al.* 2007) in between the Fraser Complex and the Yilgarn Craton would suggest that thermal reworking

did affect the margin of the craton. Fletcher *et al.* (1991) further reported a Sm–Nd isochron date of  $1291 \pm 21$  Ma for the metagabbros of the Fraser Complex, interpreted to date the crystallisation age. A Rb–Sr date of  $1268 \pm 20$  Ma on a biotite–whole-rock pair from the same gabbro, within error of the Sm–Nd date, was considered to indicate that crystallisation of the gabbro, and its emplacement at higher crustal levels along the margin of the Yilgarn Craton, happened in a relatively short time-span (Fletcher *et al.* 1991).

More recently, detailed U–Pb SHRIMP data on zircon, monazite, xenotime and rutile, and some whole-rock Sm–Nd isotopic data have enabled a more detailed picture to emerge on the development and evolution of the eastern part of the Albany Belt and the southern part of the Fraser Belt, south of 30°S (Figure 1) (Clark 1995; Nelson *et al.* 1995; Clark *et al.* 1999, 2000; Wetherley 2000; Dawson *et al.* 2002; Vallini *et al.* 2002; Bodorkos & Clark 2004a, b; Fitzsimons *et al.* 2005; Spaggiari *et al.* 2007). These data unequivocally indicate: (i) the presence of Archean basement (*ca* 2.62 Ga) along the northwest margin of the Albany–Fraser Orogen, the Munglinup Gneiss, possibly forming part of the Yilgarn Craton; (ii) the presence of a suite of granitoids aged between 1700 and 1600 Ma which do not appear to intrude but were structurally juxtaposed against the Yilgarn Craton (the Dalyup and Coramup Gneiss of the Biranup Complex); (iii) diverse episodes of deposition both on top of the Yilgarn Craton and preserved in the Albany–Fraser Orogen, mainly arenaceous sediments, with the following age ranges: >1215 Ma (Stirling Range: Rasmussen *et al.* 2002); 1790–1700 Ma (Mt Barren Group: Nelson 1996, 2001; Wetherley 2000; Dawson *et al.* 2002; Vallini *et al.* 2002); <1560 Ma (Point Malcolm paragneiss: Nelson *et al.* 1995); 1465–1305 Ma (detrital zircon in Fraser Range metasedimentary rocks: S. A. Jones unpubl. data); <1737 Ma (Woodline Formation: Hall & Jones 2005); (iv) a tectonothermal event, referred to as ‘Stage I’ tectono-metamorphism, between 1345 and 1260 Ma (Clark *et al.* 2000) relating to northwest–southeast continent–continent collision and resulting in dextral transpression; (v) minor extension and intrusion of the margin-parallel Fraser and Gnowangerup dyke swarms at *ca* 1210 Ma (Evans 1999; Wingate *et al.* 2000) and associated thermal metamorphism (Dawson *et al.* 2003); and (vi) a second convergent northwest–southeast compressive event, referred to as ‘Stage II’ tectono-metamorphism, between 1215 and 1140 Ma resulting in granitoid magmatism and emplacement of large batholiths mainly in the Nornalup Complex. Recently, Fitzsimons *et al.* (2005) reported a possible third metamorphic event from metamorphic monazite in the Mt Barren Group, which gave a U–Pb SHRIMP age of  $1027 \pm 8$  Ma. Sm–Nd isotopic data indicate a wide range of source materials including reworked Archean and Paleoproterozoic crust and juvenile mantle input with relatively short crustal residence times (Fletcher *et al.* 1991; Nelson *et al.* 1995).

In the western part of the Albany–Fraser Orogen, age data are somewhat more limited. The first robust zircon U–Pb data were reported by Pidgeon (1990), who calculated crystallisation ages of  $1289 \pm 10$  Ma for

enderbitic gneiss and ages of  $1174 \pm 12$  and  $1178$  Ma for two widely separated granitoids of what is collectively known as the Burnside Batholith. Black *et al.* (1992) expanded this work and reported zircon U–Pb SHRIMP ages between  $1198 \pm 8$  and  $1180 \pm 6$  Ma for various granitoids and associated aplitic or pegmatitic intrusions. Based on xenocrystic zircon (between 3.1 and 3.0 Ga) and  $T_{DM}$  model ages ranging from 3.05 to 1.85 Ga, Black *et al.* (1992) argued that the 1.20–1.18 Ga granitoids were derived through reworking of Archean and Paleoproterozoic protoliths. Importantly, no age equivalents to the *ca* 1.6 Ga granitoids in the eastern part of the orogen have been reported from the western portion of the Albany–Fraser Orogen.

## SAMPLING

Eight samples, collected from six localities, were separated for zircon (Figure 2). Samples FR12A2 and FR15A1 were collected from mafic orthopyroxene-bearing granulites. Samples FR16A1, FR19A1 and FR20A1 were taken from thick garnetiferous metagranitic layers within the mafic granulites. Samples FR21B1–3 were collected from an outcrop where a boudin of mafic granulite (sample FR21B2) similar to that of samples FR12A2 and FR15A1 occurs within a garnetiferous felsic K-feldspar rich granitoid (sample FR21B3), while sample FR21B1 was collected from the melt within the boudin neck (Figure 3).

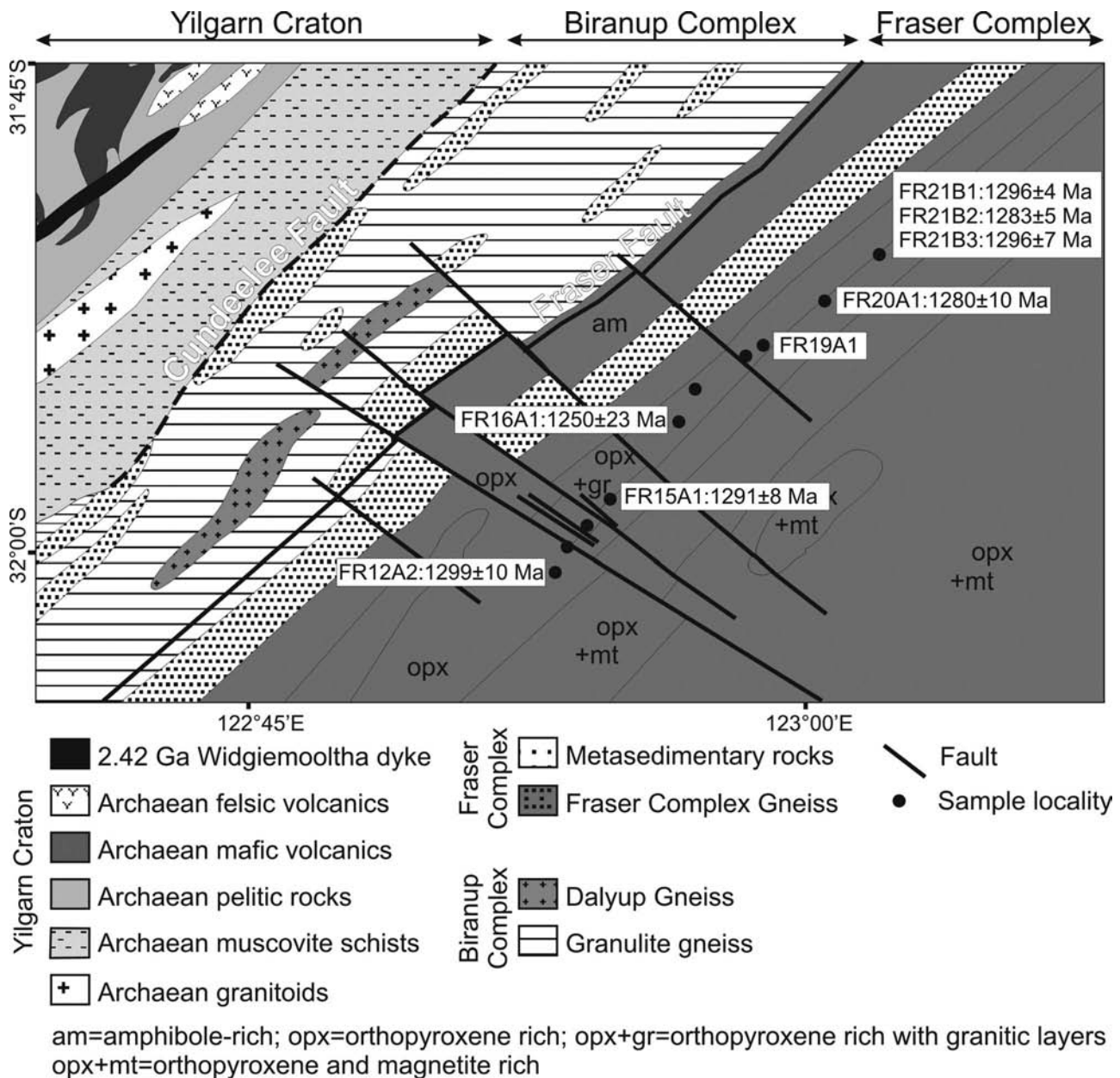


**Figure 2** Geological map of the central part of the Fraser Orogen showing sample localities and zircon U–Pb ages (based in part on Jones & Ross 2005). See Figure 1 for location.

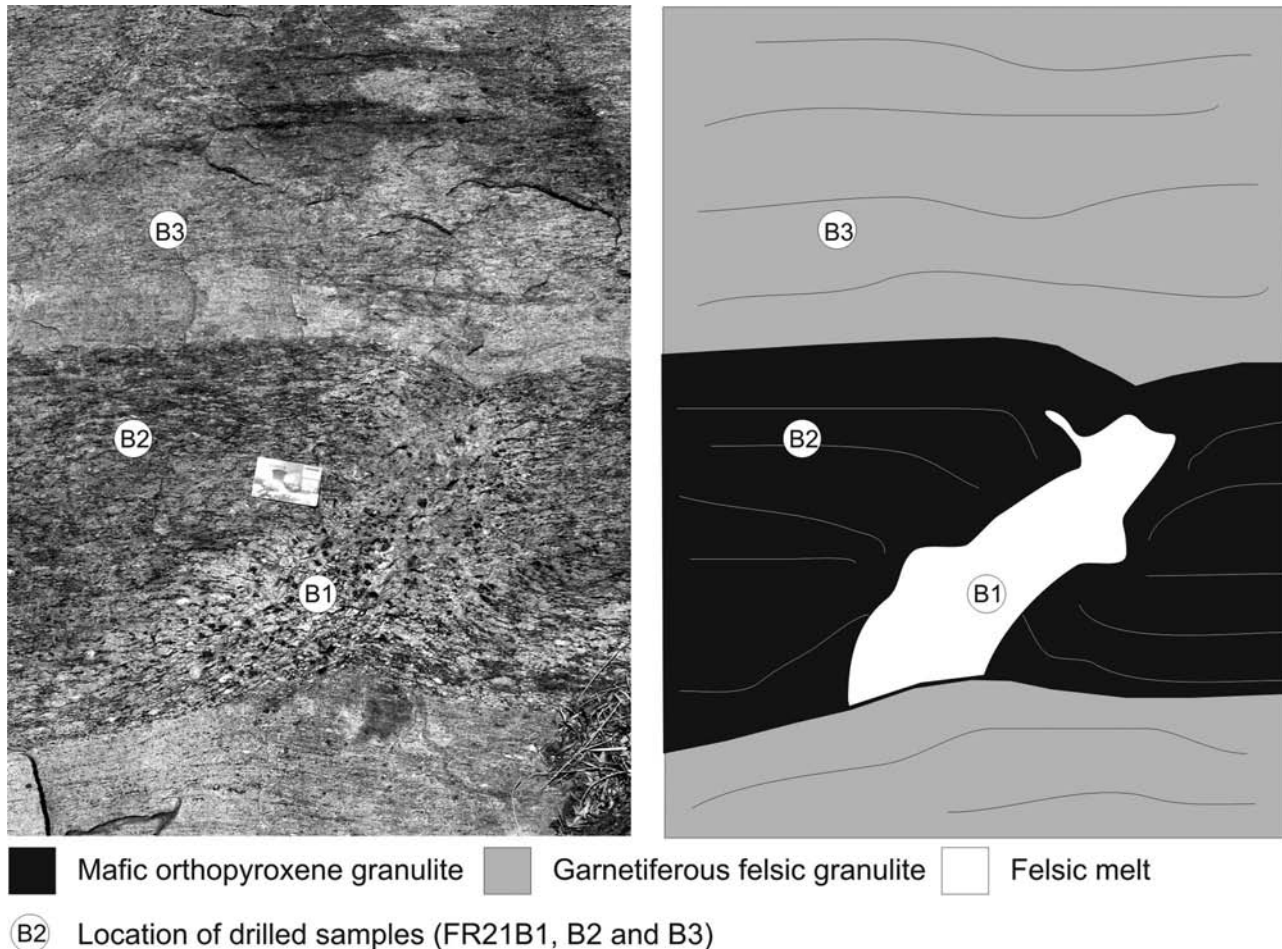


**Figure 3** Photograph and sketch of sample locality FR21B, showing a boudinaged unit of orthopyroxene-bearing mafic granulite within garnetiferous felsic granulite. Credit card used for scale.

Nineteen cores and hand samples from 13 sites (Figure 2) were collected for reconnaissance paleomagnetic and AMS studies. Block and core samples were oriented using both sun and magnetic compasses.

## METHODOLOGIES

### Zircon U–Pb geochronology

Zircon was separated from fresh rock samples through standard crushing, heavy-liquid and magnetic-separation techniques, and mounted with zircon standards in epoxy mounts. The polished mounts were C-coated for imaging on a JEOL 6400 SEM fitted with a cathodoluminescence (CL) detector to bring out internal structure (see Table 1 for zircon characteristics). The C-coating was removed, the mount thoroughly cleaned, and then re-coated with a thin Au-coat to provide conductivity. The mount was loaded in the SHRIMP sample lock 24 h before analysis, and pumped to high vacuum to allow degassing. Operating procedures of the Perth Consortium SHRIMP are detailed by Nelson (1995). Mass-positions and mass-offsets, as well as collector positions were set using zircon standard

CZ3, while the position of the  $^{204}\text{Pb}$  peak and background were monitored using doped silicate glass standard NBS 611 and a high-U metamict zircon (D23). The primary  $^{16}\text{O}_2^-$  beam operated at 2–3 nA, on a slightly elliptical spot size of 25–30  $\mu\text{m}$  during the entire session. We applied a rastering time of 2 min to remove surface contamination, and seven cycles of peak scans for a total analysis time of  $\sim 17$  min per spot. Analyses of unknowns were interspersed with zircon standard grains BR266 (Stern 2001) or TEMORA2 (Black *et al.* 2004) for which ages of 559 Ma and 418 Ma, respectively, were adopted. U content was monitored using the BR266 standards, which has 909 ppm U. Data reduction was conducted using Squid 1.09 and Isoplot 3.00 (Ludwig 2001a, b). Because the content of non-radiogenic Pb was low for all analysed zircons, and did not change noticeably throughout the course of each analysis, corrections for non-radiogenic Pb were based on measured  $^{204}\text{Pb}$  isotope and applying a common Pb composition appropriate for the age of the sample and following the two-stage model of Stacey & Kramers (1975). The data are reported in Appendix 1\*, as is the  $2\sigma$  error on the standard. This latter error is not included in age calculations, and all pooled ages are reported at the 95% confidence level.

**Table 1** Sample location and characteristics of zircon from samples of the Fraser Orogen.

Sample	Latitude	Longitude	Size ( $\mu\text{m}$ )	Aspect ratio	Shape	Cathodoluminescence (CL) response and zoning	Interpretation
FR12A2	-31.98811	122.89425	100-300	1:1-4:1	Subrounded	Low- to medium CL Broad sector zoning	Magmatic zircon
FR15A1	-31.95645	122.91741	100-300	1:1-3:1	Subrounded	Low- to medium CL; high-CL zones Broad sector zoning Small low-CL homogenous solid-state recrystallisation	Magmatic zircon
FR16A1	-31.92470	122.94431	75-200	1:1-2:1	Subrounded	Low- to high CL Oscillatory and broad sector zoning Some solid-state recrystallisation	Magmatic zircon
FR19A1	-31.89168	122.98272	50-200	1:1-3:1	Euhedral	Medium- to high-CL Oscillatory and broad sector zoning	Magmatic zircon
FR20A1	-31.87212	123.00889	50-200	1:1-4:1	Subrounded and euhedral	Low CL with some medium-CL zircon Low-CL show no zoning, medium-CL zircons have concentric zoning patterns	Magmatic zircon
FR21B1	-31.85294	123.03174	100-250	2:1-3:1	Subrounded to euhedral	Low- to medium CL Oscillatory zoning	Magmatic zircon
FR21B2	-31.85294	123.03174	100-200	1:1-2:1	Subrounded	Low- to medium CL Oscillatory zoning	Magmatic zircon
FR21B3	-31.85294	123.03174	100-300	1:1-4:1	Subrounded and euhedral	Low CL with some medium-CL zircon Oscillatory and broad sector zoning Some large low- to medium-CL sectors interpreted to reflect solid-state recrystallisation	Magmatic zircon

### Paleomagnetic analyses

Remanence composition was determined by detailed stepwise thermal demagnetisation ( $\leq 20$  steps to  $700^\circ\text{C}$ ), using a Magnetic Measurements thermal demagnetiser and the 2G-755R cryogenic magnetometer. Stepwise alternating field (AF) demagnetisation ( $\leq 26$  steps up to 160 mT) was also applied, using the 2G-600 automated degaussing system. To monitor possible mineralogical changes during heating, magnetic susceptibility was measured in selected samples after each heating step using a Bartington MS2 susceptibility meter. MS2 has also been used for AMS measurements. Magnetisation vectors were isolated using principal-component analysis (Kirschvink 1980). All vectors were defined with a minimum of four data points and a maximum angular deviation (MAD) of  $10^\circ$ .

## RESULTS

### Petrography and zircon U-Pb data

SAMPLE FR12A2: MAFIC TWO-PYROXENE GRANULITE

Sample FR12A2 was collected from a mafic two-pyroxene granulite with a granoblastic texture, which in places

shows a relict igneous texture. The clinopyroxenes clearly show exsolution lamellae, while the feldspar in places shows antiperthitic intergrowths, both indicative of relatively high-temperature metamorphism (Figure 4a-d). The absence of garnet suggests low pressures during metamorphism. Zircon grains from the sample are large, ranging in size from 100 to 300  $\mu\text{m}$ , and have aspect ratios between 1:1 and 4:1. They are colourless and clear, and have a multifaceted appearance. Cathodoluminescence (CL) imaging reveals broad sector zoning, with no indication of inherited components (Figure 5a).

Eleven analyses were conducted on 11 zircon crystals and indicated very low  $f_{206}$  values up to 0.08% (Appendix 1\*). U and Th are in the range of 160-1021 ppm and 142-1698 ppm, respectively, giving Th/U ratios between 0.71 and 1.45. The data plot close to the concordia curve (Figure 6a) and define a range of  $^{207}\text{Pb}/^{206}\text{Pb}$  ratios corresponding to a weighted mean age of  $1299 \pm 10$  Ma (MSWD = 3.8). The slight drift off concordia and low MSWD value for this population is interpreted to record some minor Pb-loss, perhaps soon after crystallisation of the zircon. The age of  $1299 \pm 10$  Ma may therefore slightly underestimate the crystallisation age of zircon in sample FR12A2 but, given the limited nature of observed Pb loss, still provides a good estimate of the crystallisation age of the sample.

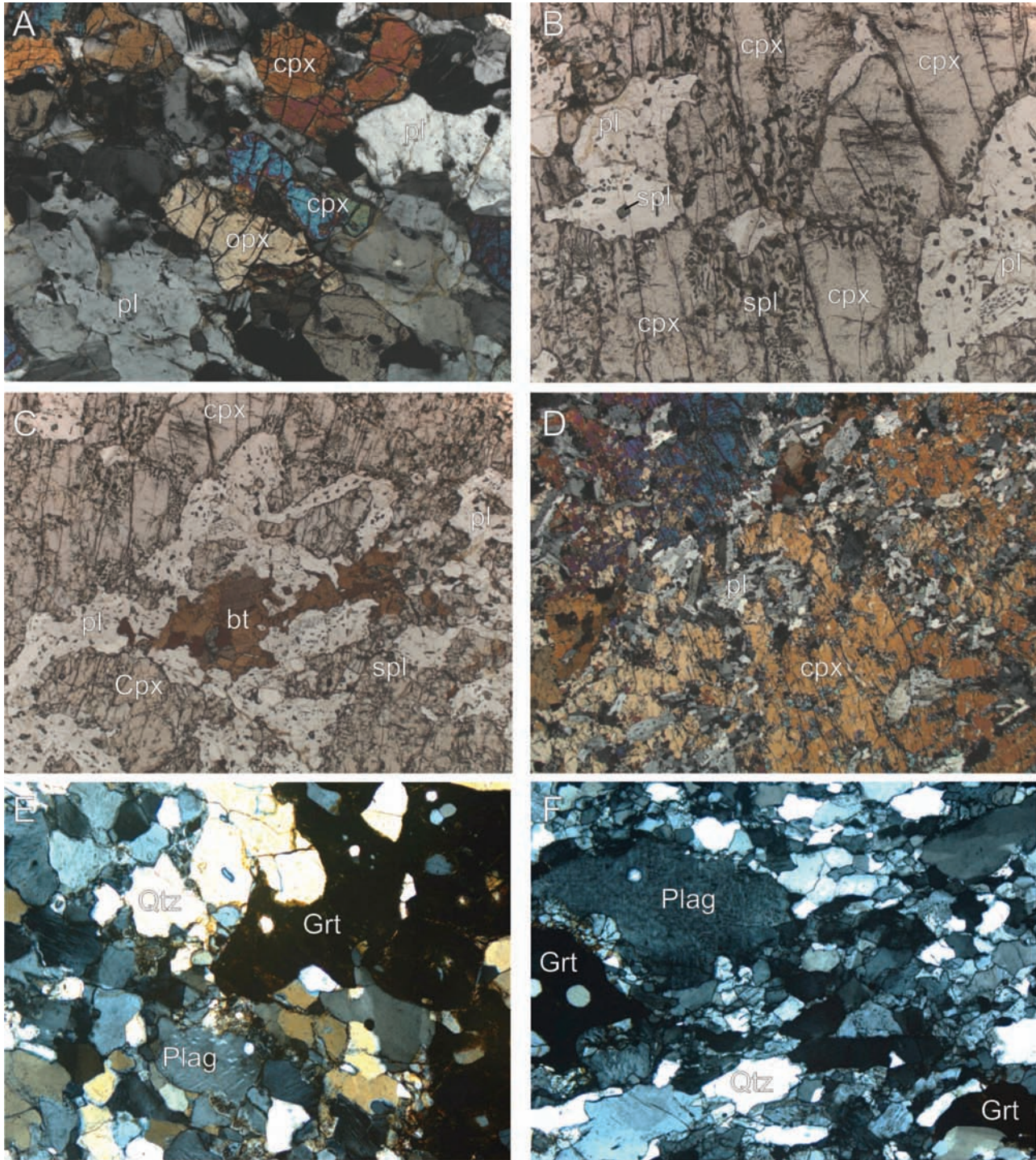


**Figure 4** (a) Two-pyroxene granulite (sample FR12A2) with assemblage clinopyroxene (cpx)–orthopyroxene (opx)–plagioclase (pl) and relict igneous texture. (b) Clinopyroxene–plagioclase granulite (sample FR13A1) with spinel (spl). (c) Clinopyroxene–plagioclase granulite with biotite (bt) replacing clinopyroxene and spinel (sample FR13A1). (d) Finer-grained portion of clinopyroxene–plagioclase granulite (FR13A2) showing relict igneous texture. (e, f) felsic garnet (grt) granulite with antiperthitic plagioclase. (field of view in a, b, c, e, f is ~3 mm; in d is ~6 mm).

#### SAMPLE FR15A1: MAFIC TWO-PYROXENE GRANULITE

Sample FR15A1 comprises a granoblastic assemblage of mesoperthitic and antiperthitic feldspar, clinopyroxene, orthopyroxene and some minor quartz. As is the case for sample FR12A2, the clinopyroxenes show exsolution

lamellae, which, together with the absence of garnet, indicate high-T and low-P conditions of metamorphism. Zircon from this sample of two-pyroxene granulite range in size from 100 to 300  $\mu\text{m}$  and have aspect ratios between 1:1 and 3:1. They are colourless to pale yellow and transparent, and display well-formed crystal faces.

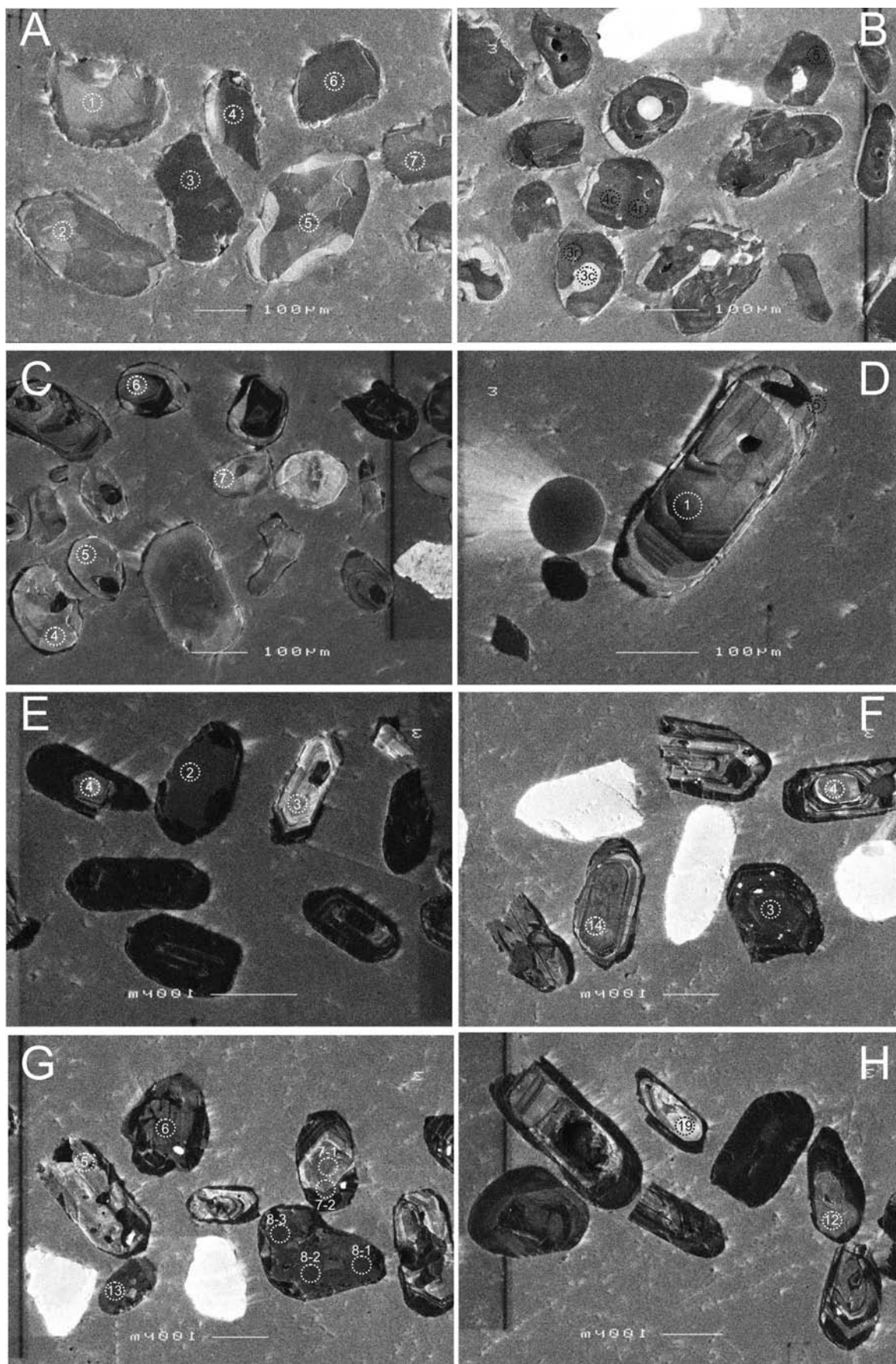


**Figure 5** Cathodoluminescence imagery of zircon from: (a) FR12A2; (b) FR15A1; (c) FR16A1; (d) FR19A1; (e) FR20A1; (f) FR21B1; (g) FR21B2; (h) FR21B3. The approximate positions of analysed spots are indicated.

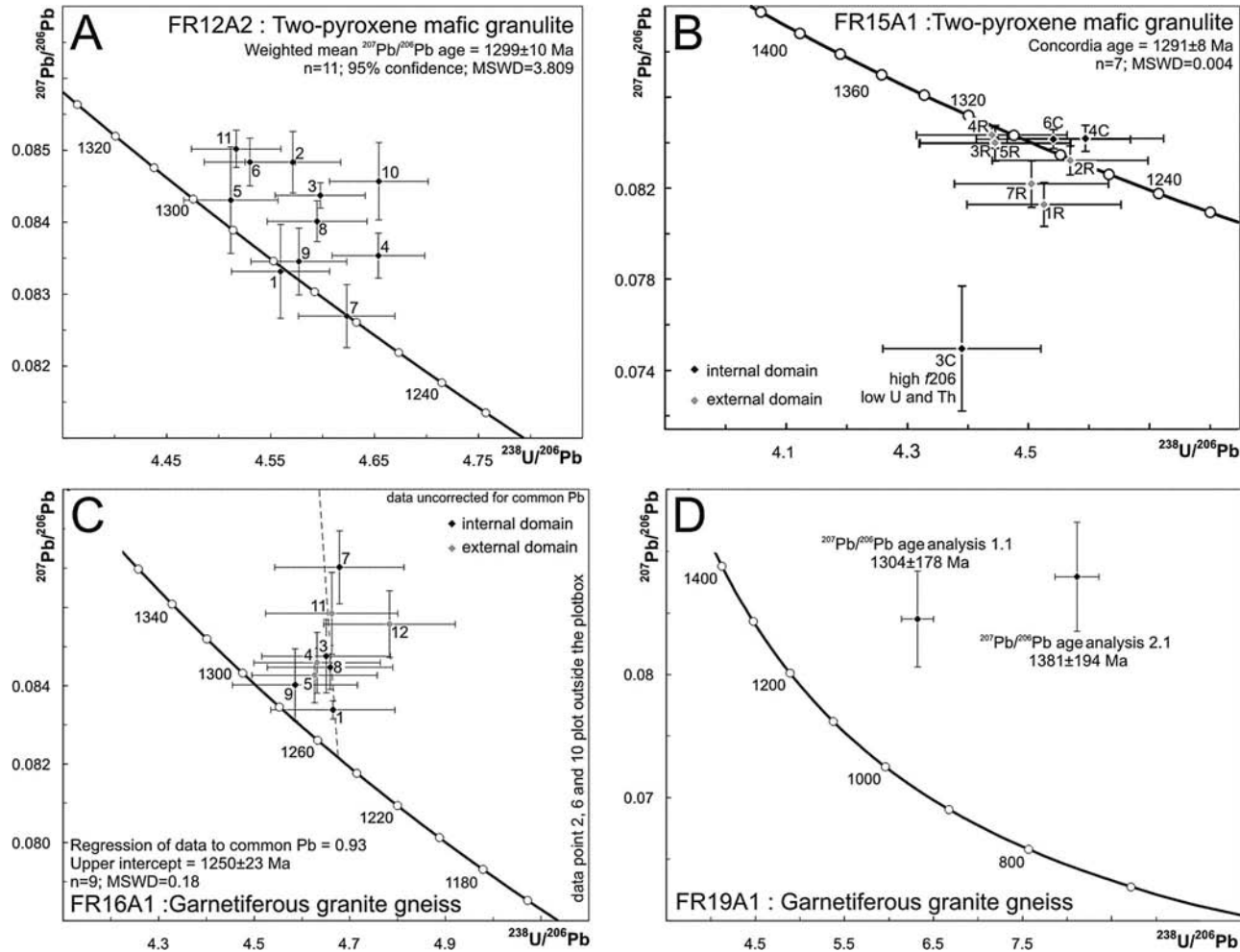


**Figure 6** U–Pb data for zircon analysed from: (a) FR12A2; (b) FR15A1; (c) FR16A1; (d) FR19A1. All error crosses are shown at  $1\sigma$  confidence level.

CL imaging indicates a low response, with some zircons showing either uniform high-response overgrowths or invasive high-CL zones interpreted to represent solid-state recrystallisation (Figure 5b).

Nine analyses were conducted on seven zircon grains, including two pairs of analyses, one in the centre and one along the rim of a single grain.  $f_{206}$  values are low, ranging from 0.04 to 0.48%, but are higher for core analysis 3, which records the lowest U and Th contents (78 and 29 ppm, respectively: Appendix 1\*). One analysis (5) records very high U and Th contents of 2328 and 3240 ppm, respectively, while the remaining analyses have U and Th contents in the range of 356–853 ppm and 160–836 ppm, resulting in Th/U ratios between 0.47 and 1.01. The low U and Th core is strongly inversely discordant, indicating overestimation of non-radiogenic Pb based on measured  $^{204}\text{Pb}$  (one count only was collected in every 2 s), and this point is therefore omitted from the calculations. The remaining data, from both core and rim, plot in a single concordant cluster (Figure 6b) that corresponds to a concordia age of  $1291 \pm 8$  Ma (MSWD of concordance = 0.0039). This indicates that all zircon crystallised within a very short time span, and the age of  $1291 \pm 8$  Ma calculated from

sample FR15A1 provides a good estimate for crystallisation of zircon in the protolith gabbro.

#### SAMPLE FR16A1: GARNETIFEROUS GRANITE GNEISS

Sample FR16A1 comprises quartz, antiperthitic feldspar, microcline, garnet and minor biotite. The rock has a granoblastic texture, and crystals are flattened to define a clear metamorphic fabric. Zircon from this sample of garnetiferous granite gneiss range in size from 75 to 200  $\mu\text{m}$  and have aspect ratios between 1:1 and 2:1. The zircon grains are colourless and clear, have well-developed crystal faces, and contain numerous small inclusions. CL imaging reveals oscillatory zoning patterns, often faded towards the rims of the crystals, interpreted to reflect solid-state recrystallisation (Figure 5c). The zircons are interpreted to be primary igneous in origin, with solid-state recrystallisation perhaps indicating a metamorphic event after crystallisation.

Twelve analyses were conducted on 12 different zircon crystals, including seven analyses on central domains, and five on external domains affected by solid-state recrystallisation. The data indicate high contents

of non-radiogenic Pb, with  $f_{206}$  values ranging from 0.07 to 15.76% (Appendix 1\*). The proportions of common Pb do not seem to be related to U and Th content, and thus are not a result of radiogenic damage and incorporation of non-radiogenic Pb in the crystal lattice. Both cores and rims show elevated contents of non-radiogenic Pb, inconsistent with the incorporation of Pb into the crystal through diffusion. The introduction of common Pb from the mount surface is discounted on the basis that none of the other samples on the same mount displayed unusual contents of common Pb. Moreover, a 2.5–3.0 min raster was applied prior to each analysis throughout the session, which would minimise surface-related common Pb. We suggest that high counts on  $^{204}\text{Pb}$  could be the result of  $\text{H}^+$  interference during the sputtering process. Assuming that the zircon grains contain significant amounts of water-bearing inclusions, volatilisation of  $\text{H}^+$  complexes could result in mass interferences that have not been adequately resolved on the SHRIMP. We therefore will treat the data for this sample as uncorrected for common Pb. U and Th are in the range of 137–636 ppm and 37–140 ppm, respectively, yielding Th/U ratios between 0.04 and 0.44. Uncorrected data plots in a tight cluster close to the concordia curve (Figure 6c), but three points, 2, 6 and 10, which yielded the highest apparent  $^{204}\text{Pb}$  contents, plot well away from the concordia. A regression of the concordant data cluster towards common Pb yields an intercept age of  $1250 \pm 23$  Ma (MSWD = 0.18) which we interpret as the best estimate of the timing of crystallisation of zircon (inner and outer domains) in sample FR16A1. The low MSWD value for this regression indicates that the solid-state recrystallisation did not affect the U–Th–Pb isotopic system significantly, or if it did, that this recrystallisation occurred immediately after crystallisation of the magmatic zircon.

#### SAMPLE FR19A1: GARNETIFEROUS GRANITE GNEISS

Sample FR19A1 contains quartz, microcline, antiperthite and minor garnet (Figure 4e, f). Only very few zircons were extracted from this garnet-bearing granite gneiss. The zircon grains range in size from 50 to 200  $\mu\text{m}$ , and have aspect ratios up to 3:1. They are yellow and transparent, and display well-developed crystal faces. CL imagery indicates prominent concentric zoning patterns consistent with crystallisation from magmatic melt (Figure 5d).

Several analyses were attempted on zircon from sample FR19A1, but were aborted due to extremely high counts on  $^{204}\text{Pb}$ . However, two analyses were completed, despite high counts on  $^{204}\text{Pb}$ , and yielded U contents of 290 and 423 ppm and Th contents of 71 and 167 ppm (Appendix 1\*). Both analyses plot well away from the concordia line (Figure 6d), but have  $^{207}\text{Pb}/^{206}\text{Pb}$  ratios allowing the calculation of apparent minimum ages of  $1304 \pm 89$  and  $1381 \pm 97$  Ma ( $2\sigma$  confidence level). Because of the highly discordant nature of these data points, and the imprecise  $^{207}\text{Pb}/^{206}\text{Pb}$  ratios due to significant correction for non-radiogenic Pb, no unbiased interpretation can be proposed for these data.

#### SAMPLE FR20A1: GARNETIFEROUS GRANITE GNEISS

Sample FR20A1 is similar in composition and texture to FR16A1 and FR19A1. Zircon from this garnetiferous granite gneiss range in size from 20 to 200  $\mu\text{m}$ , and have aspect ratios up to 4:1. The zircon crystals are yellow to yellow-brown, and range from clear to turbid, owing to variable amounts of small inclusions. The crystals are well formed, and most zircon grains have bipyramidal terminations indicative of a magmatic origin. CL imaging reveals dark to medium-CL response, with clear to faint concentric zoning patterns, as well as homogenous sectors interpreted to reflect solid-state recrystallisation (Figure 5e).

Numerous analyses were aborted after the first scan on the account of extremely high counts on  $^{204}\text{Pb}$ . Twelve analyses were completed on 12 different zircon grains, but four of those completed analyses recorded high counts on  $^{204}\text{Pb}$ , and are not further discussed here (analyses 5, 8, 11 and 12, data are reported in Appendix 1\*). Analysis 1 and 9 plot inversely discordant and correspond to analyses on high U zircon (Figure 7a). The remaining six analyses define a narrow range of  $^{207}\text{Pb}/^{206}\text{Pb}$  ratios defining a weighted mean age of  $1282 \pm 11$  Ma (MSWD = 1.2). The three most concordant data points of this set allow the calculation of a concordia age of  $1280 \pm 10$  Ma (MSWD = 0.25), which we take to represent the best age estimate for crystallisation of zircon in sample FR20A1.

#### SAMPLE FR21B1: FELSIC MELT IN THE NECK OF A BOUDIN OF TWO-PYROXENE GRANULITE

Zircon grains from sample FR21B1 range in size from 100 to 250  $\mu\text{m}$  and have aspect ratios between 2:1 and 3:1. The crystals are euhedral to subhedral, and are colourless to yellowish. CL imaging shows prominent oscillatory growth patterns consistent with growth from magmatic melt (Figure 5f).

Fifteen analyses were conducted on 12 zircons and, apart from analysis FR21B1-9-1, yielded low  $f_{206}$  values (0–0.24%: Appendix 1\*). U and Th are very variable, in the range 193–2424 ppm and 92–1707 ppm, respectively. Th/U ratios are between 0.10 and 0.75. Four data points have markedly higher  $^{207}\text{Pb}/^{206}\text{Pb}$  ratios than the main cluster, and define  $^{207}\text{Pb}/^{206}\text{Pb}$  ages between  $1674 \pm 22$  and  $1876 \pm 44$  Ma ( $2\sigma$  errors) which can be interpreted as the minimum ages of basement or detrital components incorporated in the melt as zircon xenocrysts (Figure 7b, c). The remaining 11 data points define a weighted mean  $^{207}\text{Pb}/^{206}\text{Pb}$  age of  $1294 \pm 9$  Ma, but a high MSWD value of 7.3 for this average indicates significant scatter (Figure 7b, d). Taking only the seven concordant points, a concordia age of  $1296 \pm 4$  Ma (MSWD = 3.3) can be calculated, which provides the best estimate for the crystallisation age of zircon in the melt. It is worth noting that two out of three analyses on zircon 8 form part of the concordant cluster, while one slightly discordant analysis (8-1) defines a younger  $^{207}\text{Pb}/^{206}\text{Pb}$  age of  $1238 \pm 16$  Ma. This analysis was taken from the tip of the zircon (Figure 5g), possibly indicating some

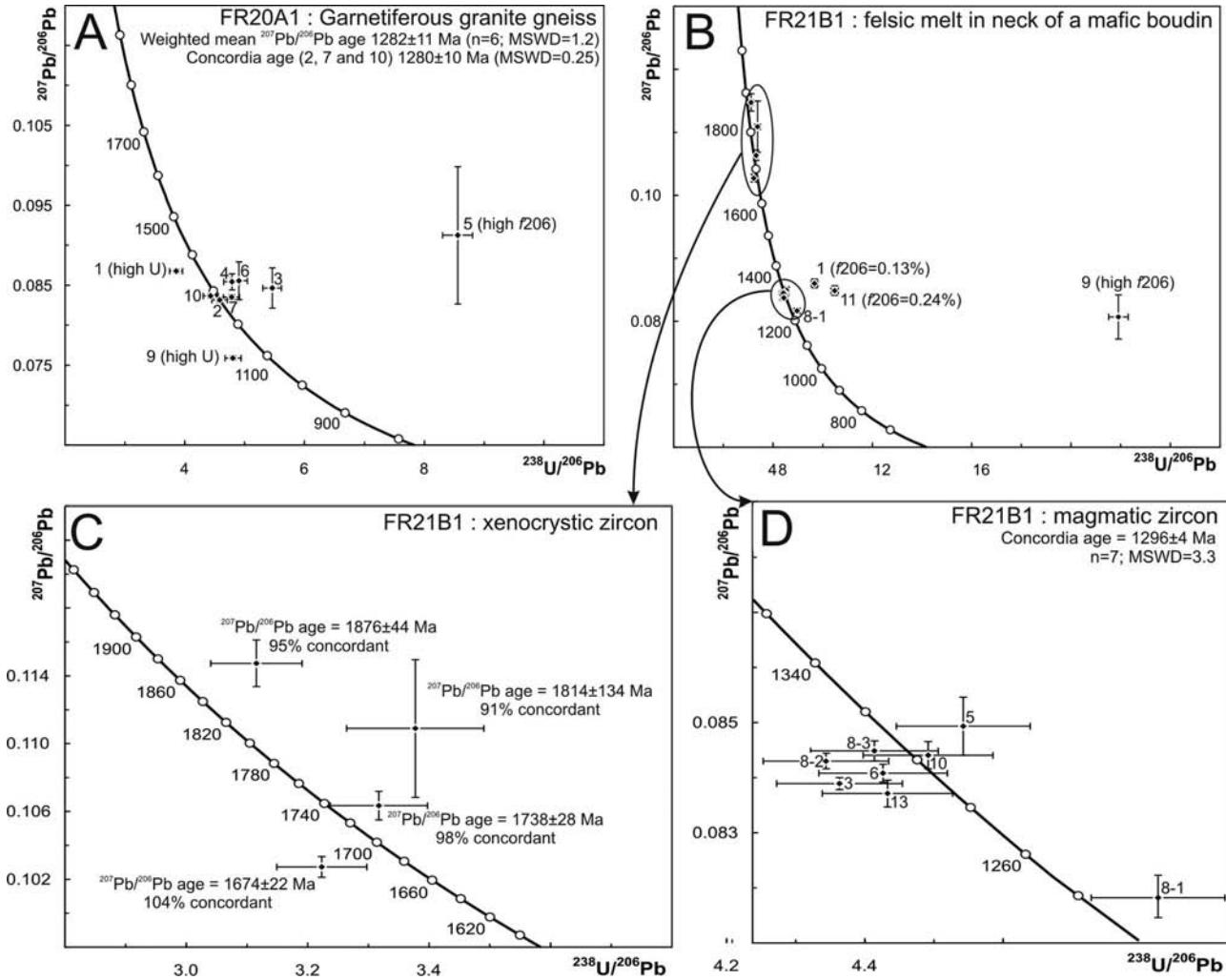


**Figure 7** U–Pb data for zircon analysed from: (a) FR20A1; (b–d) FR21B1. All error crosses are shown at  $1\sigma$  confidence level.

disturbance of the U–Th–Pb isotopic system during a metamorphic/thermal event after crystallisation of the melt.

#### SAMPLE FR21B2: MAFIC TWO-PYROXENE GRANULITE

Sample FR21B2 is similar in composition to samples FR12A2 and FR15A1 and interpreted to represent a metagabbro. This sample of mafic granulite yielded very little zircon, ranging in size between 100 and 200  $\mu\text{m}$ , and with aspect ratios up to 2:1. The few zircons that were recovered are light- to dark-yellow and have subhedral shapes. CL imaging indicates broad sector zoning indicative of a magmatic origin.

Only three zircons were successfully analysed from this sample, which appears to contain only high U zircon crystals. U and Th contents range from 1534 to 5654 ppm and from 379 to 558 ppm, respectively, giving Th/U ratios between 0.10 and 0.26. The three data points plot on concordia and define a concordia age of  $1283 \pm 5$  Ma (MSWD = 0.07), which can be taken as the crystallisation age of high-U zircon in this sample (Figure 8a).

#### SAMPLE FR21B3: GARNETIFEROUS GRANITE GNEISS

Sample FR21B3 is similar in composition and texture to FR16A1, FR19A1 and FR20A1. Zircon from this sample of garnet-bearing orthogneiss range in size from 100 to 300  $\mu\text{m}$  and have aspect ratios up to 4:1. The crystals are euhedral to subhedral, and most have well-developed terminations. The zircon grains range in colour from colourless to light yellow, and are clear. CL imaging reveals clear oscillatory zoning patterns, with some zircons showing the presence of a high-CL irregular core (e.g. zircon 19: Figure 5h).

Sixteen analyses were conducted on 15 zircons and indicate low  $f_{206}$  values up to 1.36%. Analysis FR21B3-16-1 has an anomalously high U content of 4601 ppm and was taken from a dark-CL inner sector. For the remaining analyses, U and Th values are in the ranges 68–541 ppm and 46–392 ppm, with Th/U between 0.21 and 0.94. One analysis on a high-CL irregular core (FR21B3-19-1) plots on concordia at a  $^{207}\text{Pb}/^{206}\text{Pb}$  age of  $1665 \pm 96$  Ma ( $2\sigma$  confidence), and this zircon is interpreted as a xenocryst (Figure 8b). The remaining analyses define a linear array indicating present-day Pb-loss, and a

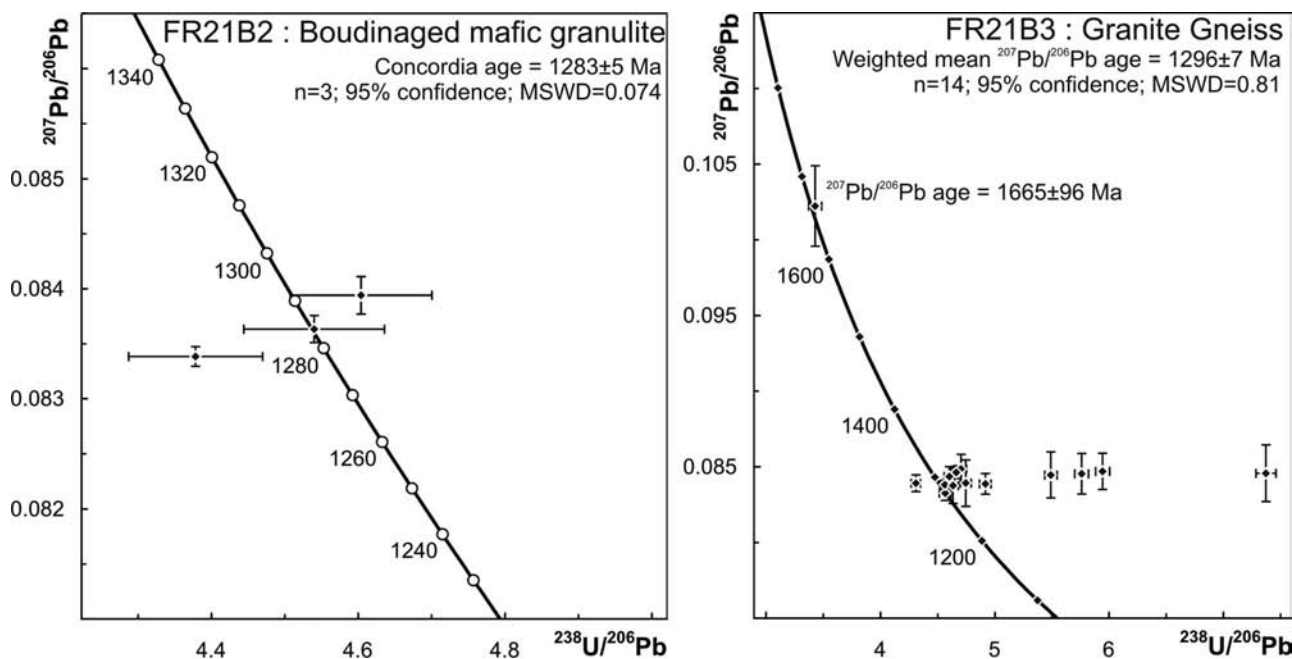


Figure 8 U–Pb data for zircon analysed from: (a) FR21B2; (b) FR21B3. All error crosses are shown at  $1\sigma$  confidence level.

weighted mean  $^{207}\text{Pb}/^{206}\text{Pb}$  age of  $1296 \pm 7$  Ma can be calculated (MSWD = 0.81), which we take as the best age estimate for crystallisation of zircon in the sample (Figure 8b).

### Paleomagnetic and AMS data

After removal of a low-stability, randomly oriented overprint from some samples, thermal and AF demagnetisations revealed two characteristic bipolar magnetisations (Figures 9, 10; Table 2). Not a single specimen contains both of these components (Figure 9).

Component 1 (FM1) is close to the BB1 component of metamorphic rocks at Bremer Bay, to the paleodirection of the Mt Barren Group metasediments, and to the Fraser Dyke remanence (Pisarevsky & Harris 2001; Pisarevsky *et al.* 2003). However, the large circle of confidence covers the large segment of the Australian Apparent Polar Wander Path (APWP) of Pisarevsky *et al.* (2003), and the FM1 pole may be slightly younger or older than those *ca* 1200 Ma poles (Figure 11). If we accept that the poles were acquired during 1.35–1.26 Ga Stage I tectonism, Australia would have remained at high latitudes and would not have moved significantly over a period of  $\sim 100$  million years. However, the high-grade multistage evolution of the Albany–Fraser Orogen is unlikely to allow the preservation of primary poles acquired during Stage I metamorphism, and we prefer to interpret the FM1 pole to reflect the paleodirection during Stage II metamorphism at *ca* 1.2 Ga.

Component 2 (FM2) resembles the BB2 component of the metamorphic rocks at Bremer Bay of uncertain age (Pisarevsky & Harris 2001). This pole lies apart from the Neoproterozoic Australian APWP (Figure 11) and we can only speculate that if this APWP will be corrected in the future by obtaining more robust *ca* 1000 Ma paleopoles with slightly more westerly longitudes, the

FM2 (BB2) pole may represent an Early Neoproterozoic remagnetisation event.

The AMS stereoplot (Figure 12) shows that the minimum axes are grouped with a mean inclination of  $4^\circ$  towards  $130^\circ$ , and maximum and intermediate axes have a ‘belt’ distribution that corresponds to a nearly vertical southwest–northeast ( $50$ – $230^\circ$ ) magnetic foliation. This is very close to the major strike of the Fraser Belt suggesting that the magnetic fabric was acquired during northwest–southeast convergence between the Yilgarn and Gawler Cratons.

## DISCUSSION

### Tectonic setting of the Fraser Complex

The Fraser Complex dominantly comprises mafic two-pyroxene granulites with relict igneous textures interpreted to represent a large metagabbro complex. These metagabbros occur side to side with felsic garnet-bearing granite gneisses. Our age data suggest that both units crystallised at about the same time, between 1.30 and 1.25 Ga, while slight disturbances of the U–Th–Pb isotopic system hint at the presence of a metamorphic/thermal event soon after crystallisation of the protoliths. Limited evidence of xenocrysts in sample FR21B3 (garnetiferous granite gneiss) and a felsic melt within the neck of a mafic boudin (sample FR21B1) are consistent with reported sources in the Fraser Belt (Woodline Formation) which contain a significant age component of 1.8–1.7 Ga (Hall & Jones 2005) and the 1.70–1.65 Ga Dalyup and Coramup Gneisses (Spaggiari *et al.* 2007). No Archean xenocrysts were recognised in the samples, suggesting that the formation of the Fraser Complex gabbro and accompanying garnet-bearing granitoids took place before docking with the Archean

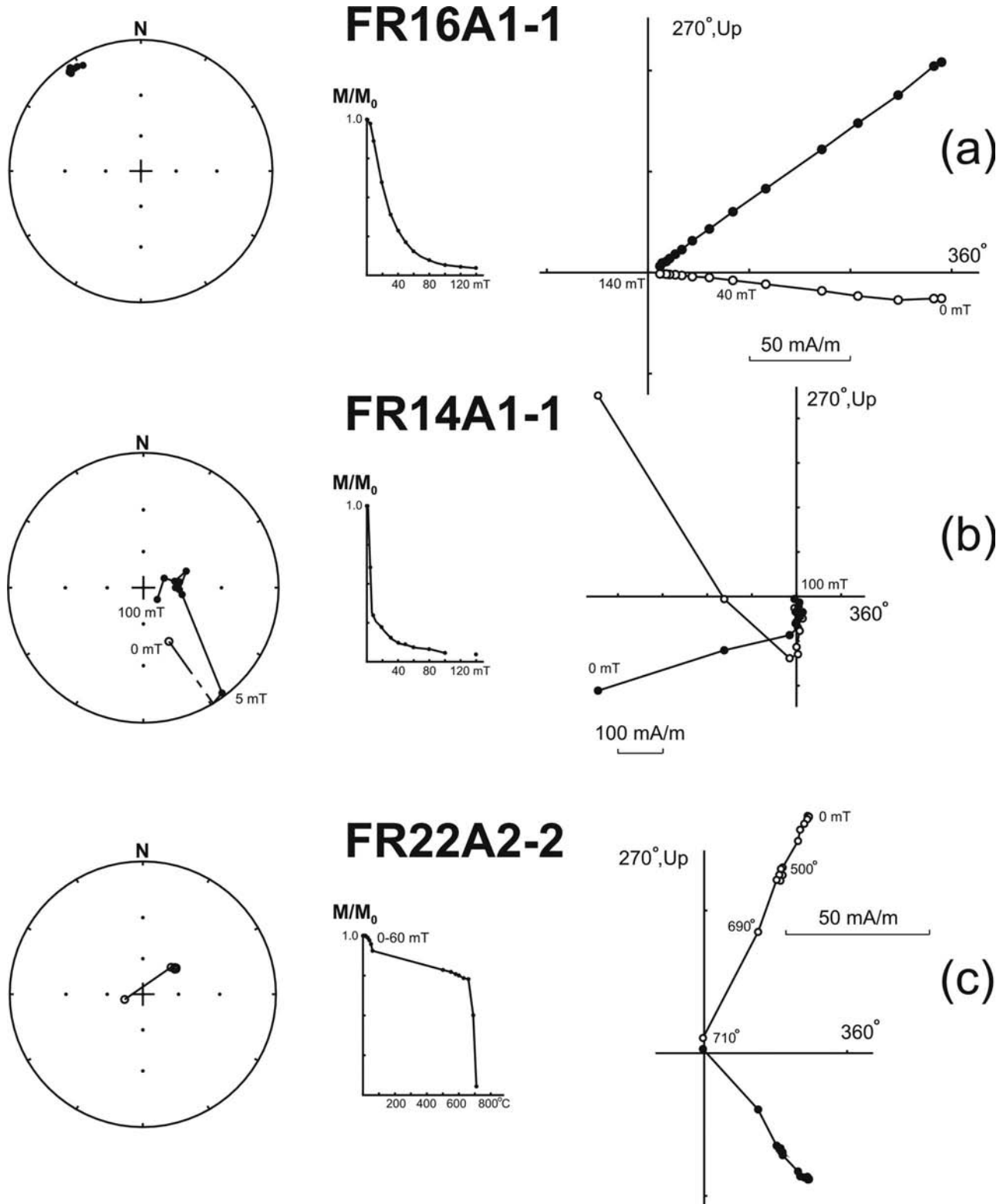


**Figure 9** Zijderveld diagrams and examples of demagnetisation behaviour for studied rocks. In orthogonal plots, open (closed) symbols show magnetisation vector endpoints in the vertical (horizontal) plane; curves show changes in intensity during demagnetisation. Stereoplots show upwards (downwards) pointing paleomagnetic directions with open (closed) symbols. (a) FR16A1-1; (b) FR14A1-1; (c) FR22A2-2.

Yilgarn Craton and/or collision between the Yilgarn and Gawler Cratons. Sm–Nd isotopic data reported for gabbros of the Fraser Complex (Fletcher *et al.* 1991)

indicate slightly negative  $\epsilon_{\text{Nd}}$  (1290 Ma) values of  $-1.7$  to  $-0.8$ , suggesting some admixing of older crust with juvenile mantle material. Such slightly negative values

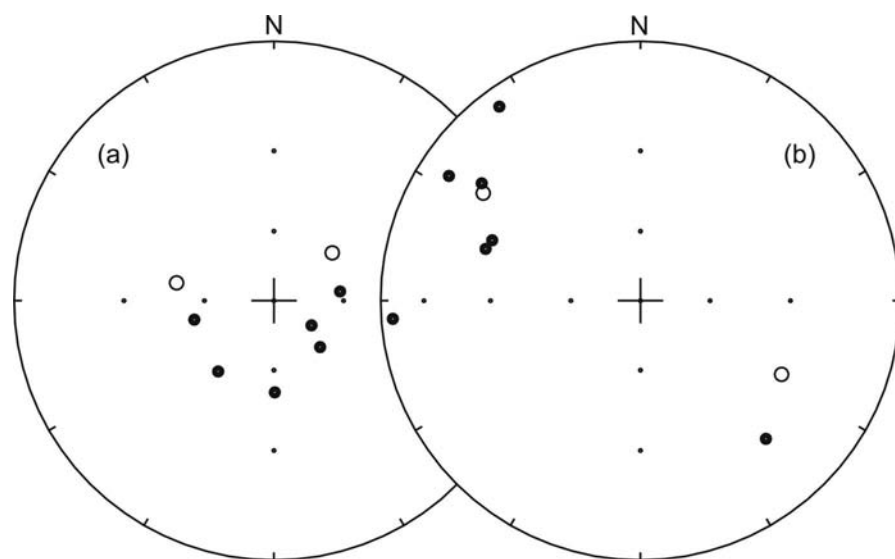


**Figure 10** Stereoplots of the directions of the characteristic remanent magnetisation from: (a) FM1; (b) FM2.

**Table 2** Mean paleomagnetic directions from metamorphic rocks of the Fraser Belt, Australia (mean coordinates 31.9°S, 122.9°E).

Component	<i>N/n</i>	Decl (°)	Incl (°)	<i>k</i>	$\alpha_{95}$ (°)	Plat (°N)	Plong (°E)	$D_p$ (°)	$D_m$ (°)
FM1	8/11	169.6	71.8	7.2	22.2	64.2	316.1	34.3	39.1
FM2	9/16	120.2	-8.6	11.3	16.0	-22.7	233.8	8.1	16.1

*N/n*, number of samples/specimens; Decl, Incl, sample mean declination, inclination; *k*, best estimate of the precision parameter of Fisher (1953);  $\alpha_{95}$ , semi-angle of the 95% cone of confidence; Plat, Plong, latitude, longitude of the paleopole;  $D_p$ ,  $D_m$ , semi-axes of the cone of confidence about the pole at the 95% probability level.

can result from some participation of a Late Paleoproterozoic crust in the melt (e.g. the 1.70–1.65 Ga Dalyup and Coramup Gneisses), or from very minor participation of Archean crust (Yilgarn Craton). The absence of Yilgarn-age xenocrysts in our samples supports the former model. Geochemical work by Condie & Myers (1999) suggested an oceanic arc origin for the Fraser Complex gabbros, but the presence of Late Paleoproterozoic xenocrysts suggests the presence of relatively juvenile microcontinental fragments, participation of which would also explain the slightly negative isotopic Nd signatures.

### Assembly of the Yilgarn and Gawler Cratons

Previous workers have identified three metamorphic events in the Albany–Fraser Orogen. Stage I metamorphism took place at between 1345 and 1260 Ma (Clark *et al.* 2000) and recorded granulite facies metamorphic conditions at 800–850°C and 500–700 MPa (Bodorkos & Clark 2004a). Stage II metamorphism took place between 1214 and 1140 Ma (Clark *et al.* 2000), and again recorded granulite facies conditions of 750–800°C and 500–600 MPa (Bodorkos & Clark 2004a). A third event has been proposed in the southwest portion of the Fraser Complex (Mt Barren Group), dated at  $1027 \pm 8$  Ma, and possibly recording upper amphibolite grade conditions (Fitzsimons *et al.* 2005). The Stage I and Stage II metamorphic evolution is interpreted to reflect northwest–southeast convergence, resulting in the juxtaposi-

tion of the Yilgarn and Gawler Cratons during Stage I, and reactivation through renewed northwest–southeast compression during Stage II. However, a slight dispersion of reliable paleopoles of mafic dykes of the dispersed ca 1070 Ma Warakurna large igneous province from the West, North and South Australian Cratons seems to suggest that the present-day configuration of the cratonic units of Australia west of the Tasman line (Figure 1, inset) only occurred after 1070 Ma (Schmidt *et al.* 2006). The relatively low pressures recorded during both Stage I and Stage II metamorphism (700 and 600 MPa, respectively; Bodorkos & Clark 2004a) suggest a crustal thickness of ~30 km, not necessarily consistent with full continental collision models. However, a recent seismic survey does indicate a present-day crustal root over 40 km thick centred ~100 km north of Bremer Bay (bb on Figure 1), the nature of which remains poorly understood (Goncharov *et al.* 2005). No kinematic models have been suggested for the contentious ca 1030 Ma ‘Stage III’ event recorded in monazite of the Mt Barren Group (mbg on Figure 1), and its tectonic significance needs further work.

### Zircon ages and metamorphism

The rocks collected as part of this study in the Fraser Complex all record granulite high-T, low-P metamorphism. However, zircon data collected from pristine oscillatory zoned magmatic zircon and from sectors

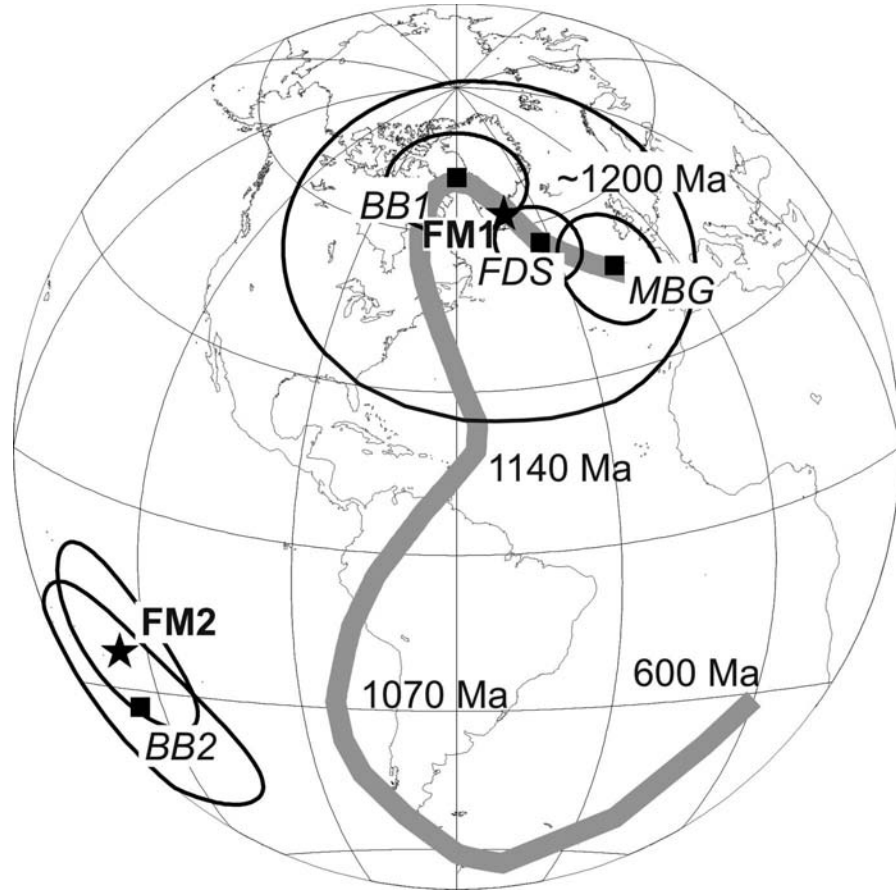


**Figure 11** Apparent Polar Wander Path for Australia between 1200 and 600 Ma (after Pisarevsky *et al.* 2003) showing the poles obtained as part of this study (FM1 and FM2) and the poles previously obtained for Bremer Bay (BB) (Pisarevsky & Harris 2001), Mt Barren (MB) and the Fraser Dyke (FDS) (Pisarevsky *et al.* 2003).

affected by solid-state recrystallisation appear to record a tight range of crystallisation ages between  $1299 \pm 10$  and  $1250 \pm 23$  Ma for both mafic and felsic units, coeval with the Stage I tectono-metamorphic event. Internal fabrics in the zircons show that most preserve a euhedral and primary magmatic character, but internal zoning is variably affected by solid-state crystallisation (Figure 5). Despite this, U–Th–Pb ratios appear relatively unaffected, suggesting that the granulite-facies conditions were characterised by very little hydrous fluids that would have allowed LILE mobility, or would have promoted crystallisation of metamorphic zircon or zircon overgrowths. Alternatively, Stage I granulite-facies metamorphism could have occurred very soon after the emplacement of the gabbros in the lower crust, resulting in overlapping magmatic crystallisation and metamorphic recrystallisation ages. The brief time-span of emplacement, subsequent granulite-facies metamorphism and exhumation into the upper crust is further supported by Rb–Sr data recording closure of the system in biotite at  $1268 \pm 20$  Ma (Fletcher *et al.* 1991).

### Magnetisation of rocks in the Fraser Complex

If we accept the presence of the multi-phase tectono-metamorphic evolution of the Albany–Fraser Orogen, with Stage I and Stage II metamorphism exceeding temperature conditions of  $750^\circ\text{C}$  (Bodorkos & Clark

2004a, b), and Stage III in the upper amphibolite facies (Fitzsimons *et al.* 2005), then the remanent magnetisation was definitely acquired during the last of these events exceeding the Curie temperature of magnetite ( $\sim 550^\circ\text{C}$ ). Given the similarity of our FM1 pole to the reported Bremer Bay, Mt Barren Group and Fraser Dyke poles (Pisarevsky & Harris 2001; Pisarevsky *et al.* 2003), assumed to record magnetisation at *ca* 1.2 Ga, it is plausible to suggest that remagnetisation of the Fraser Complex last took place during Stage II tectono-metamorphism, but further work is needed to fully resolve this issue.

### CONCLUSIONS

New zircon U–Pb data on samples from high-grade meta-igneous units of the northern part of Fraser Belt indicate that the protoliths were emplaced between  $1299 \pm 10$  and  $1250 \pm 23$  Ma. A crystallisation age of  $1296 \pm 4$  Ma on a felsic melt accumulating along the neck of a boudinaged mafic unit indicates that emplacement was very closely followed by tectonism resulting in compression along a northwest–southeast axis and accompanying extension along the northeast–southwest-oriented structural grain of the Fraser Belt. The presence, although limited, of Late Paleoproterozoic and Early Mesoproterozoic xenocrystic zircon suggests the presence of crust in the region with an age comparable

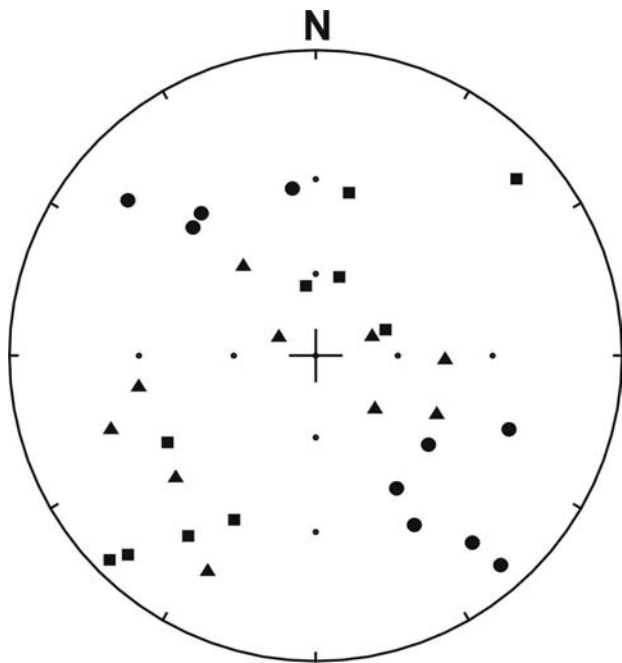


**Figure 12** Anisotropy of Magnetic Susceptibility (AMS) stereoplot. Squares, maximum axes of anisotropy; triangles, intermediate axes; circles, minimum axes.

to units in the Biranup Complex, namely the Dalyup and Coramup Gneisses, and detrital zircon in the Woodline Formation.

The dates obtained in this study correspond to Stage I tectonism as defined by Clark *et al.* (2000). Our geochronological data did not record the proposed Stage II event between 1210 and 1140 Ma of Clark *et al.* (2000), nor the reported third event at 1030 Ma (Fitzsimons *et al.* 2005). However, the paleopole FM1 obtained as part of our study is close to reported poles of *ca* 1200 Ma, suggesting that this remanence was acquired during Stage II metamorphism. It is therefore suggested that the conditions during Stage II tectono-metamorphism were probably not conducive to allow new zircon growth in the rocks of the northern part of the Fraser Complex. A second remagnetisation is recorded as pole FM2 in our rocks, suggesting a post-1.2 Ga thermal or metamorphic event affecting the northern part of the Fraser Complex. More geochronological and paleomagnetic work is needed to elucidate the age of this later event.

## ACKNOWLEDGEMENTS

We would like to acknowledge a research grant offered by the University of Western Australia for this work. SHRIMP work was carried on the Perth Consortium facilities at the John De Laeter Centre for Mass Spectrometry, Curtin University of Technology, Perth. SEM imaging was conducted at the Centre for Microscopy and Microanalysis at the University of Western Australia, Perth, and the paleomagnetic work at the Paleomagnetic Laboratory of the University of Western Australia. We also thank the staff of the

Geological Survey of Western Australia, Kalgoorlie office, for their invaluable help (especially Sarah Jones), Neal McNaughton for help with the geochronology, and journal reviewers Simon Johnson and an anonymous reviewer. BDW publishes with the permission of the Executive Director, British Geological Survey (NERC).

## REFERENCES

- BLACK L. P., HARRIS L. B. & DELOR C. P. 1992. Reworking of Archean and Early Proterozoic components during a progressive, Middle Proterozoic tectonothermal event in the Albany Mobile Belt, Western Australia. *Precambrian Research* **59**, 95–123.
- BLACK L. P., KAMO S. L., ALLEN C. M., DAVIS D. W., ALEINIKOFF J. N., VALLEY J. W., MUNDIL R., CAMPBELL I. H., KORSCH R. J., WILLIAMS I. S. & FOUDOULIS C. 2004. Improved  $^{206}\text{Pb}/^{238}\text{U}$  microprobe geochronology by the monitoring of a trace-element-related matrix effect; SHRIMP, ID-TIMS, ELA-ICP-MS and oxygen isotope documentation for a series of zircon standards. *Chemical Geology* **205**, 115–140.
- BODORKOS S. & CLARK A. J. 2004a. Evolution of a crustal-scale transpressive shear zone in the Albany–Fraser Orogen, SW Australia: 1. P–T conditions of Mesoproterozoic metamorphism in the Coramup Gneiss. *Journal of Metamorphic Geology* **22**, 691–711.
- BODORKOS S. & CLARK A. J. 2004b. Evolution of a crustal-scale transpressive shear zone in the Albany–Fraser Orogen, SW Australia: 2. Tectonic history of the Coramup Gneiss and a kinematic framework for Mesoproterozoic collision of the West Australian and Mawson cratons. *Journal of Metamorphic Geology* **22**, 713–731.
- CAMACHO A., COMPSTON W., MCCULLOCH M. T. & MCDUGALL I. 1997. Timing and exhumation of eclogite facies shear zones, Musgrave Block, central Australia. *Journal of Metamorphic Geology* **15**, 735–751.
- CAMACHO A. & FANNING C. M. 1995. Some isotopic constraints on the evolution of the granulite and upper amphibolite terranes in the eastern Musgrave Block. *Precambrian Research* **71**, 155–181.
- CAMACHO A. & MCDUGALL I. 2000. Intracratonic, strike-slip partitioned transpression and the formation and exhumation of eclogite facies rocks: an example from the Musgrave Block, central Australia. *Tectonics* **19**, 978–996.
- CLARK D. J., HENSEN B. J. & KINNY P. D. 2000. Geochronological constraints for a two-stage history of the Albany–Fraser Orogen, Western Australia. *Precambrian Research* **102**, 155–183.
- CLARK D. J., KINNY P. D., POST N. J. & HENSEN B. J. 1999. Relationships between magmatism, metamorphism and deformation in the Fraser Complex, Western Australia: constraints from new SHRIMP U–Pb zircon geochronology. *Australian Journal of Earth Sciences* **46**, 923–932.
- CLARK W. C. 1995. Granite petrogenesis, metamorphism and geochronology of the western Albany–Fraser Orogen, Albany Western Australia. BSc (Hons) thesis, Curtin University of Technology, Perth (unpubl.).
- CONDIE K. C. & MYERS J. S. 1999. Mesoproterozoic Fraser Complex: geochemical evidence for multiple subduction-related sources of lower crustal rocks in the Albany–Fraser Orogen, Western Australia. *Australian Journal of Earth Sciences* **46**, 875–882.
- DAWSON G. C., KRAPEZ B., FLETCHER I. R., MCNAUGHTON N. J. & RASMUSSEN B. 2002. Did late Palaeoproterozoic assembly of proto-Australia involve collision between the Pilbara, Yilgarn and Gawler Cratons? Geochronological evidence from the Mount Barren Group in the Albany–Fraser Orogen, Western Australia. *Precambrian Research* **118**, 195–220.
- DAWSON G. C., KRAPEZ B., FLETCHER I. R., MCNAUGHTON N. J. & RASMUSSEN B. 2003. 1.2 Ga thermal metamorphism in the Albany–Fraser Orogen of Western Australia: consequence of collision or regional heating by dyke swarms? *Journal of the Geological Society of London* **160**, 29–37.
- EVANS T. 1999. Extent and nature of the 1200 Ma Wheatbelt dyke swarm, southwestern Australia. BSc thesis, University of Western Australia, Perth (unpubl.).

- FISCHER R. A. 1953. Dispersion on a sphere. *Proceedings of the Royal Society* **A217**, 295–305.
- FITZSIMONS I. C. W. 2003. Proterozoic basement provinces of southern and southwestern Australia, and their correlation with Antarctica. In: Yoshida M., Windley B. F. & Dasgupta S. eds. *Proterozoic East Gondwana: Supercontinent Assembly and Breakup*, pp. 93–130. Geological Society of London Special Publication **206**.
- FITZSIMONS I. C. W. & BUCHAN C. 2005. Geology of the western Albany–Fraser Orogen, Western Australia—a field guide. *Geological Survey of Western Australia Record* **2005/11**.
- FITZSIMONS I. C. W., KINNY P. D., WETHERLEY S. & HOLLINGSWORTH D. A. 2005. Bulk chemical control on metamorphic monazite growth in pelitic schists and implications for U–Pb age data. *Journal of Metamorphic Geology* **23**, 261–277.
- FLETCHER I. R., MYERS J. S. & AHMAT A. L. 1991. Isotopic evidence on the age and origin of the Fraser Complex, Western Australia: a sample of Mid-Proterozoic lower crust. *Chemical Geology* **87**, 197–216.
- GONCHAROV A., PETKOVIC P., LEITCHENKOV G. & TASSEL H. 2005. Basement and crustal results from the Bremer Sub-basin, SW Australia and its Antarctic counterpart drive Australia–Russia cooperation. *Preview* **119**, 15–22.
- HALL C. E. & JONES S. A. 2005. The Proterozoic Woodline Formation: new constraints from geochronology, sedimentology and deformation studies. *Geological Survey of Western Australia Record* **2005/5**, 14–15.
- HOWARD H. M., SMITHIES R. H., PIRAJNO F., BODORKOS S. & TYLER I. M. 2005. A preliminary lithological and tectonic chronology for the west Musgrave Complex. In: Wingate M. T. D. & Pisarevsky S. A. eds. *Supercontinents and Earth Evolution Symposium*, pp. 44–45. Geological Society of Australia Abstracts **81**.
- JONES S. A. & ROSS A. A., 2005. *Yardilla, W.A. Sheet 3434, 1:100,000 Geological Series*. Geological Survey of Western Australia, Perth.
- KIRSCHVINK J. L. 1980. The least-squares line and plane and the analysis of palaeomagnetic data. *Geophysical Journal of the Royal Astronomical Society* **62**, 699–718.
- LUDWIG K. R. 2001a. Isoplot/Ex rev. 2.49, a geochronological toolkit for Microsoft Excel. *Berkeley Geochronology Center Special Publication* **1a**.
- LUDWIG K. R. 2001b. Squid 1.02: A User's Manual. *Berkeley Geochronology Center Special Publication* **2**.
- MYERS J. S. 1990. Albany–Fraser Orogen. In: *Geology and Mineral Resources of Western Australia*, pp. 255–263. Geological Survey of Western Australia Memoir **3**.
- MYERS J. S. 1993. Precambrian history of the West Australian craton and adjacent orogens. *Annual Reviews of Earth and Planetary Sciences* **21**, 453–485.
- MYERS J. S. 1995. The generation and assembly of an Archaean supercontinent: evidence from the Yilgarn craton, Western Australia. In: Coward M. P. & Ries A. C. eds. *Early Precambrian Processes*, pp. 143–154. Geological Society of London Special Publication **95**.
- NELSON D. 1995. Compilation of SHRIMP U–Pb zircon geochronology data 1994. *Geological Survey of Western Australian Record* **1995/3**.
- NELSON D. R. 1996. Compilation of SHRIMP U–Pb zircon geochronology data 1995. *Geological Survey of Western Australian Record* **1996/5**.
- NELSON D. R. 2001. An assessment of the determination of depositional ages for Precambrian clastic sedimentary rocks by U–Pb dating of detrital zircons. *Sedimentary Geology* **141/142**, 37–60.
- NELSON D. R., MYERS J. S. & NUTMAN A. P. 1995. Chronology and evolution of the Middle Proterozoic Albany–Fraser Orogen, Western Australia. *Australian Journal of Earth Sciences* **42**, 481–495.
- PIDGEON R. T. 1990. Timing of plutonism in the Proterozoic Albany Mobile Belt, southwestern Australia. *Precambrian Research* **47**, 157–167.
- PISAREVSKY S. A. & HARRIS L. B. 2001. Rock magnetic and palaeomagnetic results from high-grade metamorphic and intrusive rocks: determination of magnetic anisotropy and a 1.2 Ga palaeomagnetic pole from the Bremer Bay area, Albany Mobile Belt, Western Australia. *Australian Journal of Earth Sciences* **48**, 101–112.
- PISAREVSKY S. A., WINGATE M. T. D. & HARRIS L. B. 2003. Late Mesoproterozoic (ca. 1.2 Ga) palaeomagnetism of the Albany–Fraser orogen: no pre-Rodinia Australia–Laurentia connection. *Geophysical Journal International* **155**, F6–F11.
- RASMUSSEN B., BENGTSON S., FLETCHER I. R. & MCNAUGHTON N. J. 2002. Discoidal impressions and trace-like fossils more than 1200 million years old. *Science* **296**, 1112–1115.
- SCHMIDT P. W., WILLIAMS G. E., CAMACHO A. & LEE J. K. W. 2006. Assembly of Proterozoic Australia: implications of a revised pole for the ~1070 Ma Alcurra Dyke Swarm, central Australia. *Geophysical Journal International* **167**, 626–634.
- SPAGGIARI C. V., BODORKOS S., BARQUERO-MOLINA M. & TYLER I. M. 2007. The Yilgarn Craton meets the Albany–Fraser Orogen: Mesoproterozoic reworking of the southern craton margin. In: *Promoting the Prospectivity of Western Australia*, pp. 17–19. Geological Survey of Western Australia Record **2007/2**.
- STACEY J. S. & KRAMERS J. D. 1975. Approximation of terrestrial lead isotopic evolution by a two-stage model. *Earth and Planetary Science Letters* **26**, 207–221.
- STERN R. A. 2001. A new isotopic and trace-element standard for the ion microprobe: preliminary thermal ionization mass spectrometry (TIMS) U–Pb and electron-microprobe data. *Geological Survey of Canada Current Research Radiogenic and Isotopic Studies Report* **14-F1**.
- VALLINI D., RASMUSSEN B., KRAPEZ B., FLETCHER I. R. & MCNAUGHTON N. J. 2002. Obtaining diagenetic ages from metamorphosed sedimentary rocks: U–Pb dating of unusually coarse xenotime cement in phosphatic sandstone. *Geology* **30**, 1083–1086.
- WETHERLEY S. 2000. Tectonometamorphic evolution of the Mount Barren Group, Albany–Fraser Province, Western Australia. PhD thesis, University of Western Australia, Perth (unpubl.).
- WINGATE M. T. D., CAMPBELL I. H. & HARRIS L. B. 2000. SHRIMP baddeleyite age for the Fraser dyke swarm, southeast Yilgarn Craton, Western Australia. *Australian Journal of Earth Sciences* **47**, 309–313.

Received 5 July 2007; accepted 20 December 2007

## SUPPLEMENTARY PAPER

### APPENDIX 1: ZIRCON U–Pb SHRIMP DATA FOR SAMPLES OF THE FRASER OROGEN